Dalton Transactions

Accepted Manuscript

This article can be cited before page numbers have been issued, to do this please use: D. Bolotaulo, A. J. Metta Magana and S. Fortier, *Dalton Trans.*, 2017, DOI: 10.1039/C7DT00150A.

This is an Accepted Manuscript, which has been through the Royal Society of Chemistry peer review process and has been accepted for publication.

Accepted Manuscripts are published online shortly after acceptance, before technical editing, formatting and proof reading. Using this free service, authors can make their results available to the community, in citable form, before we publish the edited article. We will replace this Accepted Manuscript with the edited and formatted Advance Article as soon as it is available.

You can find more information about Accepted Manuscripts in the author guidelines.

Please note that technical editing may introduce minor changes to the text and/or graphics, which may alter content. The journal's standard Terms & Conditions and the ethical guidelines, outlined in our author and reviewer resource centre, still apply. In no event shall the Royal Society of Chemistry be held responsible for any errors or omissions in this Accepted Manuscript or any consequences arising from the use of any information it contains.

ROYAL SOCIETY OF CHEMISTRY

rsc.li/dalton

ROYAL SOCIETY OF CHEMISTRY View Article Online
DOI: 10.1039/C7DT00150A

Journal Name

ARTICLE

F-element metalated dipyrrins: Synthesis and characterization of a family of uranyl bis(dipyrrinate) complexes†

Received 00th January 20xx,
Accepted 00th January 20xx

DOI: 10.1039/x0xx00000x

www.rsc.org/

Duer Bolotaulo, Alejandro Metta-Magaña, and Skye Fortier*

Using an improved, chromatography-free dipyrrin synthesis, the α,β-unsubstituted dipyrrins [RC(C_4H_2N)$_2$H] (**2**) (R = tolyl (**2**^{tolyl}); *p*-OMe-C_6H_4 (**2**^{anis}); mesityl (**2**^{mes}); ferrocenyl (**2**^{Fc})) were isolated in good to excellent yields. Deprotonation of **2** with Na[N($SiMe_3$)$_2$] gives the alkali metal salts [Na(DME)$_n$][RC(C_4H_2N)$_2$] (**3**) which reacts with $UO_2Cl_2(THF)_3$ to give the uranyl bis(dipyrrinates) UO_2[RC(C_4H_2N)$_2$]$_2$(L) (L = THF (**4**^{R}-THF); DMAP (**4**^{R}-DMAP)) (R = tolyl, *p*-OMe-C_6H_4, mesityl, ferrocenyl). The THF adducts, **4**^{R}-THF, are unstable in aromatic and nonpolar solvents, rapidly decomposing to **2** and an intractable, uranium-containing solid. On the other hand, the DMAP adducts, **4**^{R}-DMAP, are indefinitely stable in solution. The solid-state structures of **4**^{R}-THF and **4**^{R}-DMAP reveal distorted trigonal bipyramidal geometries. In the solid-state, the dipyrrinate ligands exhibit significant distortions including bowing and, in some instances, out-of-plane equatorial *N*-atom coordination, likely as a consequence of steric crowding and interligand repulsion. The complexes, **4**^{R}-DMAP, have been fully characterized by NMR, UV/Vis, and fluorescence spectroscopies and their electrochemical properties investigated through cyclic voltammetry. The cyclic voltammograms of **4**^{R}-DMAP display several redox features but present in all is a reversible wave at ca. -1.9 V (vs $Fc^{0/+}$) attributable to a ligand centred reduction. Fluorescence measurements on all compounds reveal that only the mesityl derivatives **2**^{mes}, **3**^{mes}, and **4**^{mes} fluoresce, with modest Stokes shift that ranges from ca. 30 – 70 nm, with **4**^{mes} displaying the greatest relative emission intensity.

Introduction

Dipyrrins, also known as dipyrromethenes amongst a host of other names,[1] are a well-studied class of hemiporphyrinoids.[1, 2] These highly conjugated molecules are prized for their novel chemical and luminescent properties, features which can be finely tuned through chemical means owing to their high synthetic modularity and ease of functionalization.[1, 2] Accordingly, dipyrrins have received much attention for their use as intermediates in porphyrin syntheses but are perhaps best known as precursors to 4,4-difluoro-4-bora-3a,4a-diaza-s-indacene (BODIPY) dyes. Through their dipyrrin core, BODIPYs exhibit excellent properties such as stability in a wide range of temperature and pH conditions, absorption and emission modularity, and high quantum yields.[3, 4] As such, BODIPY dyes are widely used in bioluminescence imaging and labeling,[5] as laser dyes,[6] and in photoelectric applications.[7]

Not surprisingly, the chemistry of dipyrrins on transition and main group metals has also been explored to a significant extent.[1, 2, 8-10] Upon deprotonation of the pyrrolic N-H proton, dipyrrins form monoanionic, bidentate ligands which typically generate air-stable and robust metal complexes upon ligation.[8] Owing to the chemical versatility and photoproperties bestowed by the dipyrrinate ligand, these compounds have been utilized in a variety of applications such as catalysis,[11] as light harvesting arrays,[10] and as components in metal organic frameworks.[12, 13]

Considering the unique characteristics of the dipyrrin ligand, especially its utility as a chromophore for photophysical applications, there is an apparent paucity of *f*-element based dipyrrinate compounds in the literature. This is surprising given the luminescent properties of the *f*-elements and the intense study of lanthanide porphyrins and chromophores for optical materials.[14-18] While BODIPY has been used as a light harvesting and sensitizing substituent in luminescent lanthanide complexes,[19] to the best of our knowledge, only one example of an *f*-element dipyrrinate complex is known. Recently, during the course of our study, Love et al. reported the synthesis and characterization of the uranyl dipyrrinate $UO_2Cl(L')$ (L' = {(C_6F_5)C[C_4H_2N(CHN^{t}Bu)]$_2$}$^-$), featuring a donor-expanded, tetradentate dipyrrin.[20] Notably, the redox non-innocence of the ligand in $UO_2Cl(L')$ mediates electron transfer to the metal centre to effect the challenging reduction of the UO_2^{2+} unit.

In an effort to further explore and develop the dipyrrinate chemistry of the *f*-block elements, we herein report the synthesis of a series of uranyl bisdipyrrinates, $UO_2(dipy)_2(L)$ (L = THF, DMAP). In contrast to typical dipyrrin metalation procedures, these complexes have been synthesized using an anhydrous, anaerobic salt-

Department of Chemistry, University of Texas at El Paso, El Paso, Texas 79968, United States. E-mail: asfortier@utep.edu

† Electronic supplementary information (ESI) available: NMR, IR, UV/vis, and emission spectra; electrochemical data, solid-state figures and X-ray data. CCDC 1526402-1526405. For ESI and crystallographic data in CIF or other electronic format see DOI: 10.1039/x0xx00000x

metathesis route between $UO_2Cl_2(THF)_3$ and Na(dipy) to give the products in good yields. The compounds have been fully characterized, and their solid-state structures, electrochemical properties, and spectroscopic features are detailed.

Results and discussion

Ligand Synthesis

To adequately accommodate two dipyrrinate ligands within the uranyl equatorial plane, α,β-unsubstituted dipyrrins were chosen to minimize potential steric clashing between the ligands. The dipyrromethanes $[RCH(C_4H_2NH)_2]$ (**1**) (R = tolyl (**1**^{tolyl}); *p*-OMe-C_6H_4 (**1**^{anis}); mesityl (**1**^{mes}); ferrocenyl (**1**^{Fc})) and their dipyrrin derivatives $[RC(C_4H_2N)_2H]$ (**2**) (R = tolyl (**2**^{tolyl}); *p*-OMe-C_6H_4 (**2**^{anis}); mesityl (**2**^{mes}); ferrocenyl (**2**^{Fc})), substituted only in their *meso* positions, were selected to assess the potential electrochemical and luminescent effects of the backbone substituent on the uranyl complexes.

Initially, the dipyrromethanes **1** were synthesized using standard condensation methods by the trifluoroacetic acid catalysed reaction of an aldehyde with 2 equiv of pyrrole.[21, 22] This protocol necessitates the use of a vast excess of pyrrole, typically as both reagent and solvent, to disfavour oligomerization and often requires column chromatography for product purification. Regardless, in our hands, we found this procedure to be complicated by the removal of the excess pyrrole and the formation of tri- and oligopyrrane by-products. Additionally, the α,β-unsubstituted dipyrromethanes **1** are highly acid sensitive when dissolved in solution, and the reaction must be carried out quickly to prevent decomposition (visually indicated by the transformation of the pale yellow solution to a red/green mixture).

In an effort to avoid these synthetic issues, an alternative method was sought. Using a modified procedure developed by Dehaen et al.,[23] **1** can be synthesized in modest to good yields by using acidified water (ca. 0.18 M HCl) as the carrier solvent. Under these conditions, only a slight excess of pyrrole (3 equiv) is required as the insoluble dipyrromethane product precipitates from solution, preventing further oligomerization. The crude dipyrromethane is readily isolated by filtration and can be further purified by sublimation or recrystallization from toluene, obviating the need for chromatography.

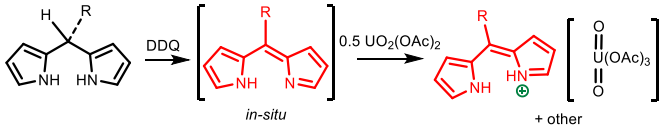

Scheme 1. Attempted *in-situ* synthesis of $UO_2(dipy)_2$ and isolation of dipyrrinium uranyl triacetate.

With **1** in hand, the synthesis of uranyl bis(dipyrrinate) was attempted using established one-pot procedures for dipyrrin metalation, namely the in-situ oxidation of **1** to **2** followed by addition of a metal acetate or halide under ambient conditions.[8, 10, 24] Treatment of a pale yellow, CH_2Cl_2 solution of **1**^{tol} with 2,3-dichloro-5,6-dicyano-1,4-benzoquinone (DDQ) generates a dark red mixture consistent with the formation of **2**^{tol}. Subsequent addition of 0.5 equiv of $UO_2(CH_3COO)_2{\cdot}2H_2O$ gives a complicated product mixture from which a single crystal was eventually isolated. Analysis by X-ray crystallography revealed the formation of [H**1**^{tol}][$UO_2(CH_3COO)_3$] (Scheme 1). The dipyrrinium uranyl acetate salt presumably forms by the protonation of **2**^{tol} with CH_3COOH, generated in the reaction, to give [H**1**^{tol}][CH_3COO] which further complexes with unreacted $UO_2(CH_3COO)_2$ starting material. The formation of dipyrrinium salts in this fashion has been previously documented by Cohen et al. and can be remedied by the use of a base to trap the acid product generated in the reaction.[8] However, following attempts in the presence of excess NEt_3 as base proved equally unsuccessful, prompting us to explore better defined, step-wise routes.

In particular, we envisioned that the targeted uranyl bis(dipyrrinates) could be accessed through salt metathesis between a uranyl halide and an alkali metal dipyrrinate. Consequently, this first required the synthesis and isolation of the free dipyrrins, **2**, which can be easily synthesized by the treatment of a toluene solution of **1** with DDQ in the presence of NEt_3.[10, 25] Upon work up, this affords a dark red-brown oil which crystallizes upon standing in cold hexanes. In this manner, we have found column chromatography is not needed for purification. Interestingly, free dipyrrins are purported to be difficult to isolate or unstable compounds;[8, 24, 26] however, **2** was readily isolated in good yields as pure compounds with no decomposition observed when stored under ambient conditions after several months.

Treatment of **2** with $NaN(SiMe_3)_2$ cleanly gives the sodium dipyrrinates $[Na(DME)_n][RC(C_4H_2N)_2]$ (R = tolyl (**3**^{tolyl}), n = 0.3; *p*-OMe-C_6H_4 (**3**^{anis}), n = 0.75; mesityl (**3**^{mes}), n = 0; ferrocenyl (**3**^{Fc}), n = 0) in 76-90% yields after recrystallization. These compounds have been fully characterized by spectroscopic techniques and elemental analyses. While alkali metal derivatives of dipyrrinates are known,[27, 28] to the best of our knowledge, compounds **3** are the first example of α,β-unsubstituted, alkali metallated dipyrrins. When kept under strictly anhydrous and anaerobic conditions, **3** can be stored indefinitely both as a solid and in solution.

Uranyl Dipyrrinate Synthesis

The reaction of $UO_2Cl_2(THF)_3$ with **3** in THF generates a deep red solution from which the uranyl dipyrrinates $UO_2[RC(C_4H_2N)_2]_2(THF)$ (**4**-THF) (R = tolyl (**4**^{tolyl}-THF); *p*-OMe-C_6H_4 (**4**^{anis}-THF); mesityl (**4**^{mes}-THF); ferrocenyl (**4**^{Fc}-THF)) can be isolated as dichroic red-green microcrystalline solid upon filtration and removal of the solvent (Scheme 2). In all cases, slow diffusion of pentane into concentrated THF/DME solutions of **4**-THF kept at -30 °C affords red-green crystalline material.

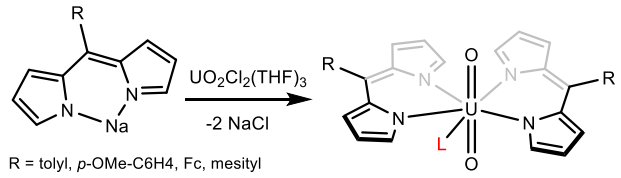

Scheme 2. Synthesis of uranyl bis(dipyrrinates) **4**-THF and **4**-DMAP via salt metathesis.

The solid-state structures of **4**-THF (*vide infra*) reveal the uranium adopts an approximate pentagonal bipyramidal structure formed by the two axial oxo groups and, in the equatorial plane, two dipyrrinates with one bound molecule of THF, giving the complexes an overall C_{2v} symmetry. In solution, however, the ^{1}H NMR spectra of **4**-THF in C_6D_6/THF-d_8 or pyridine-d_5 (py-d_5) is not consistent with this geometry as it features a truncated peak set indicative of higher symmetry. This suggests that the coordinated THF is labile in solution and exhibits a rapid on/off equilibrium, providing an averaged D_{2h} symmetry on the NMR time scale, or completely dissociates to give six-coordinate $UO_2(dipy)_2$ (**4**). Surprisingly, and in support of the former, **4**-THF is only stable in

View Article Online
DOI: 10.1039/C7DT00150A

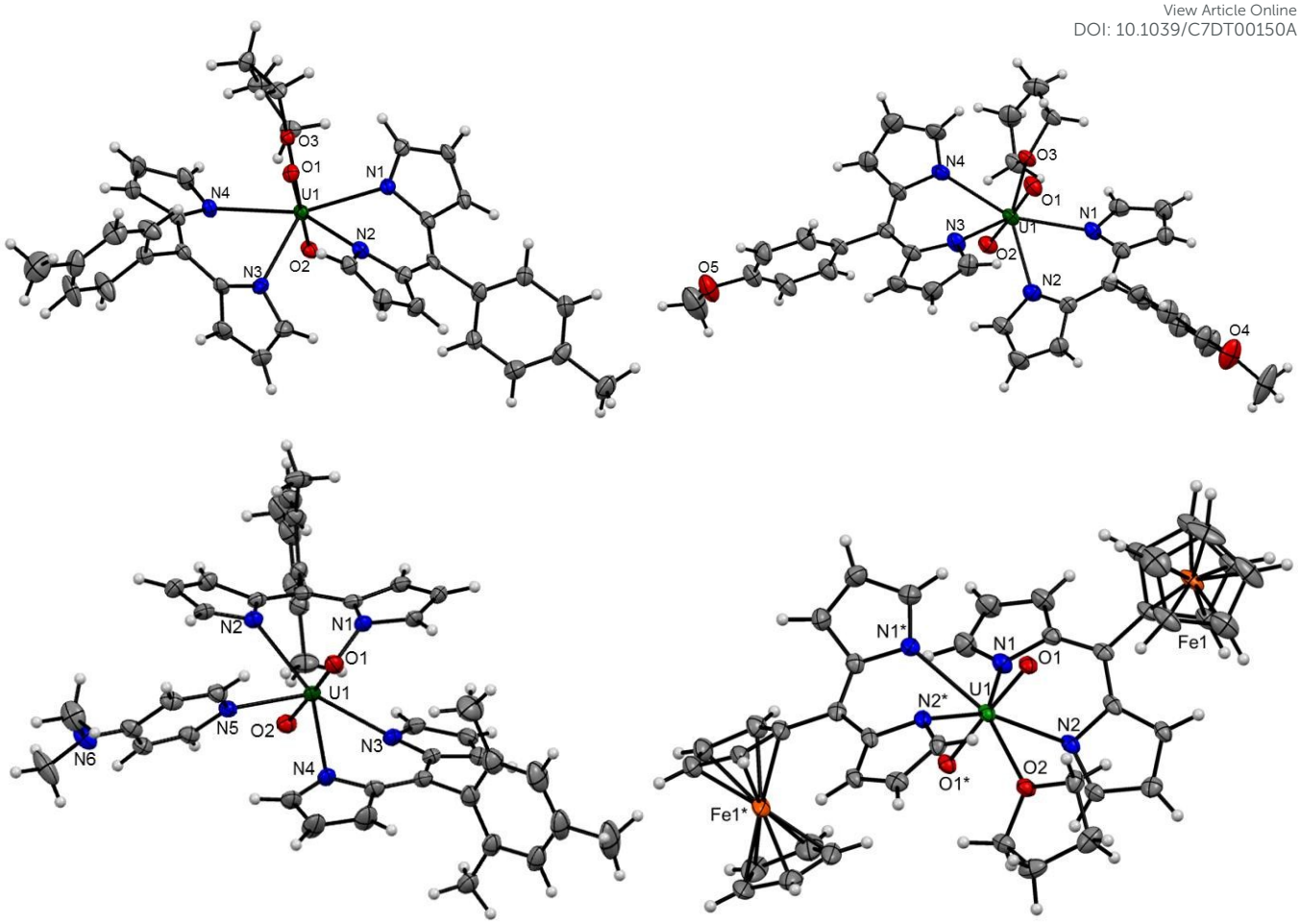

Figure 1. Solid-state structures of 4^{tolyl}-THF·3THF, 4^{anis}-THF·THF·C_5H_{12}, 4^{Fc}-THF·C_5H_{12}, and 4^{mes}-DMAP·THF·0.5C_5H_{12} (top left, clockwise). Co-crystallized solvent molecules omitted for clarity. Asterisks denote symmetry generated atoms.

the presence of coordinating solvents as it immediately decomposes in aromatics to give **2** and an as of yet unidentified, intractable uranium containing precipitate – a transformation visually marked by a colour change from deep red to brown. Moreover, the ^{1}H NMR spectra of crystalline **4**-THF is always marked by the appearance of free dipyrrin **2** in varying amounts, regardless of the preparation method. The inherent solution-phase instability of **4**-THF and the ubiquity of **2** in all samples precluded further product characterization.

In an attempt to improve the stability of **4** by disfavouring solvent loss through use of a superior σ-donor, 4-dimethylaminopyridine (DMAP) was added as a coordinating base in the uranyl dipyrrinate syntheses to give $UO_2[RC(C_4H_2N)_2]_2$(DMAP) (**4**-DMAP) (R = tolyl (4^{tolyl}-DMAP); *p*-OMe-C_6H_4 (4^{anis}-DMAP); mesityl (4^{mes}-DMAP); ferrocenyl (4^{Fc}-DMAP) in excellent yields (Scheme 2). These DMAP adducts are sparingly soluble in toluene and aliphatics, partially soluble in benzene and Et_2O, and fully soluble in polar solvents such as THF or DME. When dissolved, **4**-DMAP maintains a dark red colour in solution that appears solvent independent. More notably, **4**-DMAP does not decompose in these solutions.

In the solid-state, the pentagonal bipyramidal $UO_2(dipy)_2(L)$ geometry is maintained as represented by the structure of 4^{mes}-DMAP (*vide infra*). Regardless, the ^{1}H NMR spectra of **4**-DMAP in C_6D_6 (with a drop of py-d_5 for solubility) again shows a set of resonances in line with D_{2h} symmetry. It must be noted, though, that the ^{1}H NMR spectrum of 4^{Fc}-DMAP at room temperature in C_6D_6/py-d_5 displays a persistent set of minor resonances in an approximate 3:1 ratio, indicative of the presence of a second isomeric form. Variable temperature ^{1}H NMR spectroscopic measurements were carried out to further elucidate the nature of the isomeric mixture (Figure S29). Upon cooling a C_7D_8/py-d_5 solution of 4^{Fc}-DMAP to -30 °C, the isomeric ratio decreases to 2:1. At room temperature, the non-Cp resonances of the minor isomer are poorly resolved but sharpen at low temperature, revealing a multitude of peaks consistent with C_{2v} symmetry. Upon warming to 80 °C, the ^{1}H NMR spectrum simplifies through coalescence of the resonances towards the major isomer. Taken together, this spectral data can be explained by an equilibrium shift in which DMAP binding to the uranyl becomes favourable at lower temperatures while its lability increases at higher temperatures.

Attempts to synthesize the solvent-adduct-free form of **4** in the absence of a coordinating base were unsuccessful, giving **2** as the only identifiable product.

Solid-State Characterization of 4-THF and 4-DMAP

As noted, crystals of **4**-THF can be readily grown from the slow diffusion of pentane into concentrated THF/DME solutions. Single crystals of 4^{tolyl}-THF, 4^{anis}-THF, and 4^{Fc}-THF were found suitable for X-ray crystallographic analysis while single crystals of the mesityl derivative were isolated as its DMAP adduct, 4^{mes}-DMAP. In all cases, the single crystals appear red with a green sheen.

The complexes crystallize as the solvates **4**^{tolyl}-THF·3THF, **4**^{anis}-THF·THF·C_5H_{12}, **4**^{Fc}-THF·C_5H_{12}, and **4**^{mes}-DMAP·THF·0.5C_5H_{12} in the triclinic, trigonal, and monoclinic space groups $P\bar{1}$, $P\bar{1}$, $P\bar{3}1c$, and $P2_1/c$, respectively. Both **4**^{tolyl}-THF·3THF and **4**^{anis}-THF·THF·C_5H_{12} feature two, full independent uranyl molecules in their asymmetric units with each of the pairs exhibiting similar structural features. In **4**^{Fc}-THF·C_5H_{12}, the uranyl lies on a crystallographic special position through which the full molecule is generated by symmetry. The solid-state structures of **4**^{tolyl}-THF·3THF, **4**^{anis}-THF·THF·C_5H_{12}, **4**^{Fc}-THF·C_5H_{12}, and **4**^{mes}-DMAP·THF·0.5C_5H_{12} are shown in Figure 1.

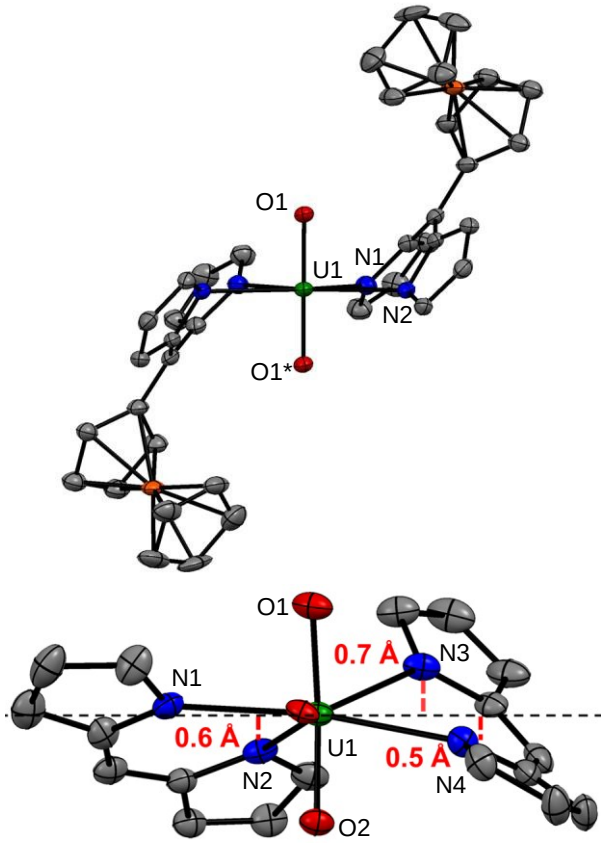

Figure 2. Truncated solid-state structures of **4**^{Fc}-THF·C_5H_{12} (top) and **4**^{tolyl}-THF·3THF (bottom) showing out of plane bonding and *N*-atom displacement, respectively. Select atoms omitted for clarity. Asterisk denotes symmetry generated atom.

In the solid-state, the uranyl bis(dipyrrinates) exhibit a distorted pentagonal bipyramidal geometry. In order to accommodate the coordinated THF or DMAP in the fifth equatorial position, the dipyrrinates are pushed towards one another. Consequently, this distorts the U-N_{dipy} bonds giving rise to inequivalent U-N bond lengths for each ligand, i.e. one short (ca. 2.45 Å) and one long (ca. 2.55 Å). Nonetheless, the U-N_{dipy} bond distances of **4** (U-N = 2.458(5) – 2.526(6) Å (**4**^{tolyl}-THF); 2.453(4) – 2.547(5) Å (**4**^{anis}-THF); 2.457(4) Å, 2.482(4) Å (**4**^{Fc}-THF); 2.473(6) – 2.555(5) Å (**4**^{mes}-DMAP)) are similar to that found in the donor-expanded dipyrrinate $UO_2Cl(L')$ (U-N = 2.465(5), 2.483(4) Å)[20] and other uranyl porphyrinoids.[29-35]

The uranium-oxo bonds (U-O = 1.768(5), 1.765(5) Å and 1.755(4), 1.758(5) Å (**4**^{tolyl}-THF); 1.759(4), 1.764(4) Å and 1.762(4), 1.762(4) Å (**4**^{anis}-THF); 1.773(3) Å (**4**^{Fc}-THF); 1.764(4) and 1.766(4) Å (**4**^{mes}-DMAP)) and the O=U=O angles (O-U-O = 177.4(2)° and 170.9(2)° (**4**^{tolyl}-THF); 176.8(2)° and 170.5(2)° (**4**^{anis}-THF); 177.0(2)° (**4**^{Fc}-THF); 176.9(2)° (**4**^{mes}-DMAP)) of **4** are unremarkable for the most part and within typical UO_2^{2+} structural parameters (U-O = 1.78 Å, O-U-O = 180°), indicating little perturbation of the uranyl moiety by the dipyrrinate ligands.[36] This is further substantiated by the IR spectra (KBr pellet) of **4**-DMAP which all display an absorption at 963 cm^{-1} attributable to the asymmetric U=O stretch, similar to that known for $[UO_2(H_2O)_5]^{2+}$ (ν_{asym} U=O = 962 cm^{-1}).[36] Tellingly, this indicates an electronic insensitivity of the UO_2^{2+} unit to the dipyrrinate backbone substituents.

Notably, though, significant distortions are observed in relation to the dipyrrinate ligands. For instance, the conjugated dipyrrin core is normally planar but it is noticeably bowed in the case of **4**. This is quantified by the dihedral angles between the pyrrolic rings in **4**^{tolyl}-THF (11.1°, 20.5° and 27.3°, 31.0°), **4**^{anis}-THF (8.5°, 20.8° and 29.6°, 29.6), **4**^{Fc}-THF (37.2°), and **4**^{mes}-DMAP (20.4°, 22.3°); however, the bond distances within the ligands appear otherwise unaffected. Additionally, the dipyrrinate ligands bend out from the equatorial plane in **4**^{tolyl}-THF (42.5°, 43.2° and 27.3°, 43.3°), **4**^{anis}-THF (43.58°, 44.5° and 41.2°, 24.7°), **4**^{mes}-DMAP (44.6°, 40.1°), and **4**^{Fc}-THF (59.9°) as illustrated in Figure 2 (top).

A further manifestation of the ligand distortion appears in the form of out of plane, *N*-atom displacement in some of the solid-state structures. For example, one of the molecules in **4**^{tolyl}-THF·3THF (Figure 2, bottom) shows three of the *N*-atoms sitting out of the equatorial mean plane at a distance of 0.5 – 0.7 Å. This deviation is unusual for uranyl, which typically adheres to strictly bipyramidal geometries, but has been reported in a few instances in complexes with other *N*-donor ligands.[36-40] While crystal packing forces may play some role, these structural phenomena are best explained as a consequence of sterics. Inspection of the spacefilling models of the uranyl bis(dipyrrinates) clearly show ligand crowding that necessitates the observed bowing and twisting in order to avoid intramolecular, interligand clashing with the forward-pointing α-hydrogen atoms of the dipyrrinates (Figure S37).

Electrochemistry

Dipyrrins are well-known to be redox active molecules, capable of one-electron reduction or oxidation, where the potentials and reversibility is substituent dependent.[1, 28, 41, 42] In the case of $UO_2Cl(L')$, the dipyrrinate ligand plays an integral part in the reduction chemistry of the metal centre, facilitating the two-electron reduction of U(VI) to U(IV).[20] As such, the electrochemical features of the uranyl bis(dipyrrinate) complexes were investigated by cyclic voltammetric analysis.

The cyclic voltammograms (CVs) of **4**-DMAP are feature rich, exhibiting a varying range of complexity between each complex (see Supporting Information). Nevertheless, each CV displays a shared set of three reduction waves that appear from ca. -1.9 to -2.9 V vs $Fc^{0/+}$ (cf Figure 3). Of the three reductions, only the first wave exhibits any reversibility, coming in at $E_{1/2}$ = -1.91, -1.88, -1.96, and -1.96 V for **4**^{tolyl}-DMAP, **4**^{anis}-DMAP, **4**^{Fc}-DMAP, and **4**^{mes}-DMAP, respectively. Comparison of this feature to the reversible reduction wave found in **2**^{anis} ($E_{1/2}$ = -1.96 vs $Fc^{0/+}$) (Figure 3, top and Figure

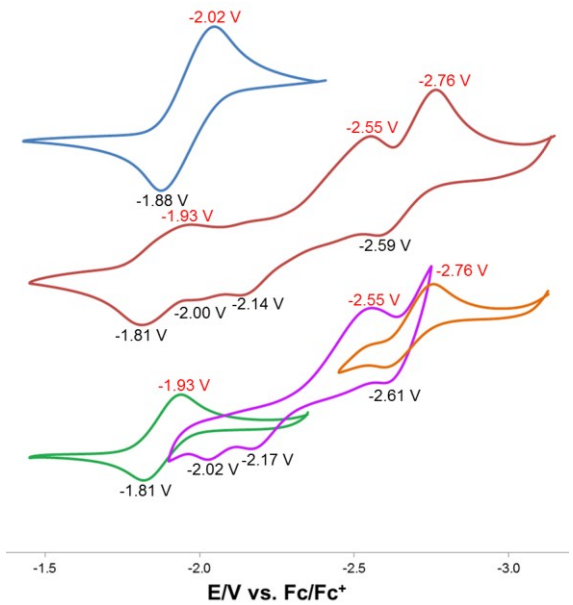

Figure 3. Cyclic voltammogram of $\mathbf{2}^{anis}$ (top, blue) and $\mathbf{4}^{anis}$-DMAP (middle, red) with its deconvoluted traces (bottom) in THF at a scan rate of 0.25 V s^{-1} (0.1 M $[NBu_4][PF_6]$ as supporting electrolyte).

S60) show this redox event to be ligand based, similar to that found for other metal dipyrrinates.[28]

The subsequent irreversible reduction waves for **4**-DMAP, appearing at ca. –2.0 and –2.9 V, share qualitative similarities to the reduction features in the CV of $UO_2[N(SiMe_3)_2]_2(THF)_2$ (Figure S62) and fall at the lower edge of reduction potentials for uranyl complexes with *N*-donor ligands (ca. -1.8V vs $Fc^{0/+}$).[36] However, the CV of $\mathbf{2}^{anis}$ (Figure S60) also shows two irreversible reduction waves within this potential window. Thus, the origin of these reductions, whether ligand or metal based or a combination thereof, is not readily discernible.

Finally, in the case of $\mathbf{4}^{Fc}$-DMAP, a reversible oxidation wave is observed at $E_{1/2}$ = 0.07 V vs $Fc^{0/+}$ (Figure S58) assignable to the Fe(II)/Fe(III) redox couple of the ferrocenyl moiety, similar in feature to that observed for free ferrocene. As such, the CV of $\mathbf{4}^{Fc}$-DMAP shows an electrochemically rich system with promising ligand and metal based redox chemistry.

Electronic Absorption and Fluorescence Spectroscopy

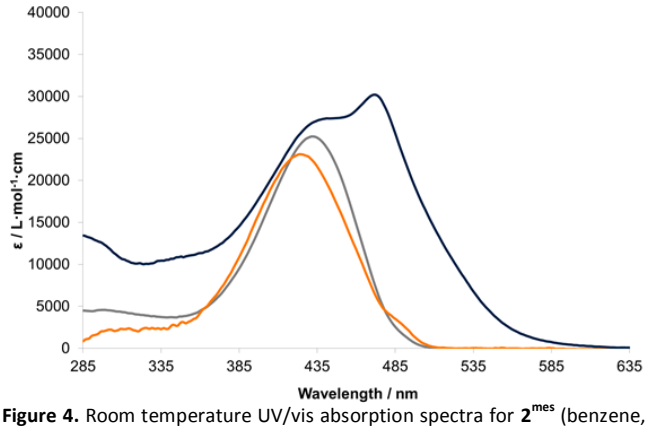

Figure 4. Room temperature UV/vis absorption spectra for $\mathbf{2}^{mes}$ (benzene, 25.1 µM, C_6H_6) (orange), $\mathbf{3}^{mes}$ (9.66 µM, C_6H_6) (grey), and $\mathbf{4}^{mes}$**DMAP** (12.9 µM, C_6H_6) (black).

The photophysical properties of the dipyrrin systems **2**, **3**, and **4** in benzene were examined by UV-vis spectroscopy. The spectra of **2** are typical for dipyrrins and show maximum absorbances between 436 to 456 nm (ε = 18,959 – 24,385 $L{\cdot}mol^{-1}{\cdot}cm^{-1}$) consistent with $\pi \rightarrow \pi^*$ transitions (see Figure 4 and Supporting Information).[13] Interestingly, the deprotonation of **2** to **3** has little to no significant effect on the electronic absorption spectra of these compounds (cf Figure 4). Yet, upon complexation to uranyl, a number of changes are observed. At first glance, the molar absorptivity is observed to increase in **4**-DMAP over those of **2** and **3**. Yet, as each uranyl complex features two dipyrrinate ligands, the molar absorptivity per dipyrrinate in **4**-DMAP is actually diminished in comparison (e.g., $\mathbf{2}^{Fc}$ (ε = 20,412 $L{\cdot}mol^{-1}{\cdot}cm^{-1}$) *vs* $\mathbf{4}^{Fc}$-DMAP (ε = 13,789 $L{\cdot}cm^{-1}$ per mole dipyrrinate)). Additionally, a new band appears in $\mathbf{4}^{tolyl}$-DMAP, $\mathbf{4}^{anis}$-DMAP, and $\mathbf{4}^{mes}$-DMAP giving a different bathochromically shifted maximum absorbance at 462 (ε = 35,416 $L{\cdot}mol^{-1}{\cdot}cm^{-1}$), 467 (ε = 34,826 $L{\cdot}mol^{-1}{\cdot}cm^{-1}$), and 472 nm (ε = 30,214 $L{\cdot}mol^{-1}{\cdot}cm^{-1}$), respectively (cf Figure 4). While sharpening or splitting of the dipyrrin absorbance bands has been observed upon metalation,[10, 13] the absorption spectra show no appreciable change in the physiognomy of the dipyrrin peaks in **4**-DMAP. This new band cannot be attributed to the UO_2^{2+} moiety alone as uranyl, while photoactive, absorbs at λ_{max} = 414 nm (ε = ca. 11 $L{\cdot}mol^{-1}{\cdot}cm^{-1}$) with lower intensity.[43] Thus, we have tentatively assigned this new band as arising from a dipyrrin to uranium ligand-to-metal charge transfer (LMCT).

Given the luminescent properties of dipyrrins and their derivatives, fluorescence measurements were undertaken. The excitation wavelengths were set to the respective UV/vis absorption maxima obtained in the same solvent (C_6H_6) using comparable concentrations. It should be noted that solvent polarity can have a profound effect on the fluorescence of metal dipyrrinate complexes,[25] but this phenomenon was not investigated in our systems. Of the twelve dipyrrin complexes studied, it was found that only the mesityl derivatives $\mathbf{2}^{mes}$, $\mathbf{3}^{mes}$, and $\mathbf{4}^{mes}$-DMAP fluoresce and their emission spectra is shown in Figure 5. It is well-

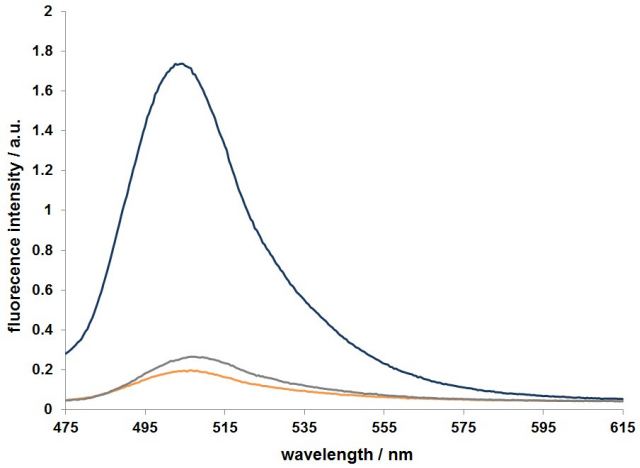

Figure 5. Emission spectra of $\mathbf{2}^{mes}$ (orange), $\mathbf{3}^{mes}$ (grey),and $\mathbf{4}^{mes}$-DMAP (black), as 10 µM solutions in C_6H_6 at room temperature after excitation at 453, 432, and 472 nm, respectively. The emission wavelengths are 505, 507, and 504 nm for $\mathbf{2}^{mes}$, $\mathbf{3}^{mes}$,and $\mathbf{4}^{mes}$-DMAP, respectively.

established that aryldipyrrinates with mesityl groups in the *meso* position display enhanced fluorescence due to torsional constriction, increasing rigidity and thus minimizing competitive non-radiative decay pathways.[1, 2, 25, 44] The spectra in Figure 5 show a modest Stokes shift that ranges from ca. 30 – 70 nm, in line with that found for other metalated dipyrrinates.[2] Notably, while **2**^{mes} and **3**^{mes} exhibit similar emission intensities, the relative fluorescence of **4**^{mes}-DMAP is nearly an order of magnitude greater in comparison (Figure 5), indicating a marked interaction between uranyl and the dipyrrinate ligands.

Conclusion

Dipyrrins are popular and versatile chromophores that have received much attention for their use in BODIPY dyes and luminescent metal complexes; however, their chemistry with *f*-elements has been glaringly underexplored. This may be due to synthetic challenges as attempts to use standard dipyrrin metalation procedures failed in our case to generate uranyl dipyrrinates. Gratifyingly, we have shown that the uranyl bis(dipyrrinates) $UO_2[RC(C_4H_2N)_2]_2$(DMAP) (**4**-DMAP) can be readily accessed through an anhydrous, salt metathesis route, opening a new pathway to lanthanide and actinide dipyrrinate chemistry. The new compounds were fully characterized and shown to exhibit a number of salient structural and spectral features. For instance, the emission spectrum of **4**^{mes}-DMAP demonstrates that dipyrrin fluorescence can be enhanced upon complexation to uranyl. Efforts to further expand the dipyrrinate chemistry of uranium and other *f*-elements are currently underway in our laboratory.

Experimental

General Considerations.
All air and moisture-sensitive operations were performed in a M. Braun dry box under an atmosphere of purified nitrogen or using high vacuum standard Schlenk techniques. Benzene, toluene, hexanes, pentane, toluene, THF, Et_2O, and dimethoxyethane (DME) were dried using a Pure Process Technology Solvent Purification System and subsequently stored under a dinitrogen atmosphere over activated 4 Å molecular sieves. All deuterated solvents were purchased from Cambridge Isotope Laboratories Inc. and were degassed by three freeze–pump–thaw cycles and dried over activated 4 Å molecular sieves for 24 h prior to use. Celite and 4 Å molecular sieves were heated to 200 °C for at least 24 h and then cooled under vacuum. Ferrocenecarboxaldehyde and $UO_2Cl_2(THF)_3$ were prepared according to literature procedures.[45, 46] All other reagents were purchased from commercial sources and used as received. NMR spectra were recorded on a JEOL ECA 600 MHz or a Bruker AVANCE III 400 MHz spectrometer. Resonance assignments in the ^{13}C NMR spectra were based upon ^{1}H – ^{13}C HMQCGP 2D correlation spectra. ^{1}H NMR and ^{13}C NMR spectra are referenced to $SiMe_4$ using the residual ^{1}H solvent peaks as internal standards or the characteristic ^{13}C resonances of the solvent. IR data were collected using a Thermo Scientific Nicolet iS5 spectrometer. UV-vis spectra were recorded on a Shimadzu UV-3101PC UV-vis/NIR scanning spectrophotometer. All analyte concentrations were set to 10 μM in benzene or as otherwise noted. Fluorescence spectra were recorded using an Olis DM45 spectrofluorimeter with a 150 W Xe Arc lamp. For the fluorescence measurements, the excitation wavelength was set to the absorption maxima of each compound determined from their UV-vis absorption spectra. All analyte concentrations were set to 10 μM in benzene. Elemental Analyses were performed by Robertson Microlit Laboratories, Inc. and Midwest Microlabs, LLC.

Cyclic Voltammetry.
Cyclic voltammetric measurements were performed using a CH Instruments 600e potentiostat with a PC unit controlled with CHI software (version 13.12). Experiments were performed in a glovebox under an inert N_2 atmosphere using platinum disks (2 mm diameter) embedded in Kel-F thermoplastic as the counter and working electrodes while the reference electrode consisted of a platinum wire. Solutions utilized in the electrochemical studies were approximately 1 mM in complex with $[NBu_4][PF_6]$ (0.1M, THF) as supporting electrolyte. All potentials are reported versus the $[Cp_2Fe]^{0/+}$ couple, referenced as internal standard.

X-ray Crystallography.
Data for **4**^{tolyl}-THF·3THF, **4**^{anis}-THF·THF·C_5H_{12}, **4**^{Fc}-THF·C_5H_{12}, and **4**^{mes}-DMAP·THF·0.5C_5H_{12} were collected on a Bruker 3-axis platform diffractometer equipped with an APEX I CCD detector using a graphite monochromator with a Mo Kα X-ray source (λ = 0.71073 Å). The crystals were mounted on a glass fiber or on a Mitigen Kapton loop, coated in NVH oil, and maintained at 100(2) K under a flow of nitrogen gas during data collection. A hemisphere of data was collected using ω and ϕ scans with 0.5° frame widths. Data collection and cell parameter determinations were conducted using the SMART program.[47] Integration of the data and final cell parameter refinement were performed using SAINT[48] software with data absorption correction implemented through SADABS.[49] Structure solution, refinement, graphics, and creation of publication materials were performed using SHELXTL[50] or the Olex2 crystallographic package.[51] Structures were solved using direct, charge flipping, or structure expansion methods and difference Fourier techniques. The co-crystallized pentane molecules in **4**^{anis}-THF·THF·C_5H_{12}, **4**^{Fc}-THF·C_5H_{12}, and **4**^{mes}-DMAP·THF·0.5C_5H_{12} exhibit positional disorder which was addressed by modeling the disordered atoms over several orientations. All hydrogen atom positions were idealized and treated as riding on the parent atom. A summary of relevant crystallographic data is presented in Table S1.

General procedure for the chromatography-free synthesis of α,β-unsubstituted aryldipyrromethanes (1)
The following is a modified procedure adapted from published methods.[23] In a 500 mL round bottom flask equipped with a large magnetic stir bar, deionized water (250 mL) was degassed using three freeze-pump-thaw cycles. To the water was added HCl(aq) (3.7 mL, 12 M), to acidify the solution, under an atmosphere of dinitrogen. Freshly distilled pyrrole (3 equiv) was added and the solution was vigorously stirred. To this, 1 equiv of arylaldehyde was added very slowly dropwise at an approximate rate of 0.5 mL/h. Upon immediate addition of the arylaldehyde, the solution turns opaque. The subsequent drop was added only after precipitation of a fine white to pale yellow solid accompanied by a decrease in turbidity. It is important to note that vigorous stirring and slow addition of aldehyde are critical for ease of workup and increased yields and purity. Upon complete addition of the arylaldehyde, a saturated aqueous solution of $NaHCO_3$ (200 mL) was added. The supernatant was then decanted and the precipitate was collected

on a Büchner funnel to give a pale yellow to peach coloured solid. The solid was washed copiously with deionized water (5 × 30 mL) and dried overnight under vacuum. The solid was then sublimated under reduced pressure at 125 °C to yield white crystals. Alternatively, storage of a concentrated toluene solution of the aryldipyrromethanes at -10 °C gives the product as a white coloured precipitate. In our hands, the aryldipyrromethanes were observed to be indefinitely stable as solids under ambient conditions. The products **1**^{tol}, **1**^{anis}, **1**^{mes}, and **1**^{Fc} were characterized by ^{1}H and ^{13}C{^{1}H} NMR spectroscopy and their identity confirmed by comparison to reported values.[21, 52] Note: The dipyrromethanes **1** are highly acid sensitive

1^{tol}**:** 4.16 mL of pyrrole (4.02 g, 0.06 mol) was treated as described with 2.36 mL of 4-methylbenzaldehyde (2.40g, 0.02 mol). The material was purified by sublimation. Yield: 1.8 g (51%).
1^{anis}**:** 3.70 mL of pyrrole (3.31 g, 49.3mmol) was treated as described with 2 mL of 4-anisaldehyde (2.24 g, 16.4 mmol). The peach coloured product was recrystallized from toluene. Yield: 2.1g (51%).
1^{mes}**:** 2.81 mL of pyrrole (2.72 g, 40.5 mmol) was treated with 2.0 mL of mesitaldehyde (2.0 g, 13.5 mmol). The peach coloured product was recrystallized from toluene. Yield: 2.06 g (60%).
1^{Fc}**:** 2.4 mL of pyrrole (2.32 g, 34.6 mmol) was treated with 2.46 g of ferrocenecarboxaldehyde (11.5 mmol) dissolved in THF (0.5 mL). Upon addition, the solution turns cloudy and red which then fades upon formation of a fine yellow powder. Dissolution in toluene afforded an amber solution, and storage at -10°C produced a yellow-orange microcrystalline powder. Yield: 1.2 g (33%).

General procedure for the chromatography-free synthesis of α,β-unsubstituted aryldipyrromethenes (**2**)
The following is a modified procedure adapted from published methods.[10, 25] In a 250 mL round bottom flask, 1 equiv of aryldipyrromethane **1** was dissolved in toluene with vigorous stirring. Approximately 50 mL of toluene was used per gram of **1** to completely dissolve the material. A solution of 2,3-dichloro-5,6-dicyano-1,4-benzoquinone (DDQ) (1.1 equiv) in toluene (50 mL) was added all at once to the aryldipyrromethane. Upon addition, a brown precipitate is formed. The progress of the reaction was monitored by TLC (silica, Et_2OAc:Hexanes, 25:75), showing full consumption of the dipyrromethane after 3 h. Excess triethylamine (5 equiv) was added to the stirring solution to dissolve the brown precipitate. After 30 minutes, the volatiles were removed in vacuo. The product mixture was dissolved in CH_2Cl_2, and the solution was washed with saturated $NaHCO_3$ solution (1 × 50 mL), brine (1 × 50 mL), and deionized water (1 × 50 mL). The CH_2Cl_2 fraction was dried over anhydrous $MgSO_4$ and the solution was concentrated under reduced pressure, leaving the minimum amount of solvent necessary to keep the product dissolved. The brown solution was added dropwise to a stirring solution of hexanes (75 mL) which caused the precipitation of a fine, grey-brown precipitate. The solid was removed via filtration through Celite supported on a medium porosity glass frit. Concentration of the filtrate and storage of the solution at -10 °C for 24 h produces the dipyrromethene as a pure material. The α,β-unsubstituted aryldipyrromethenes were stored under ambient conditions and observed to be unchanged after several months. The products **2**^{tol}, **2**^{anis}, and **2**^{mes} were characterized by ^{1}H and ^{13}C{^{1}H} NMR spectroscopy and their identity confirmed by comparison to reported values.[10, 23]

2^{tol}**:** 0.55 g (2.3 mmol) of **1**^{tol} was treated as described with 0.58 g (2.6 mmol) of DDQ. The crude product is an oil that can be recrystallized from storage of a concentrated hexanes solution at -10 °C to give red-amber crystals. Yield: 0.50 g (90%).
2^{anis}**:** 1.4 g (5.6 mmol) of **1**^{anis} was treated with 1.4 g (6.1 mmol) of DDQ as described in the general synthesis with minor modifications. It was found that foregoing aqueous workup dramatically increases yield. After removal of triethylamine and toluene, the reaction mixture was redissolved in neat toluene (10 mL). This solution was added dropwise to a stirring solution of hexanes (75 mL), causing the formation of a grey precipitate. The precipitate was removed by filtration and the solvent evaporated by vacuum to give **2**^{anis} as an oil. The storage of a concentrated hexanes solution at -10°C gives the product as pink-orange prismatic needles. Yield: 0.97 g (70%).
2^{mes}**:** 2.15 g (8.10 mmol) of **1**^{mes} was treated as described with 2.0 g (8.9 mmol) of DDQ. The crude product is a grey-green solid that can be recrystallized from storage of a concentrated hexanes solution at -10 °C to give dark green crystals. Yield: 1.95 g (91%).
2^{Fc}**:** 1.23 g (3.70 mmol) of **1**^{Fc} was treated as described in the general synthesis with 0.93g (4.1 mmol) of DDQ with minor modifications. It was found that foregoing aqueous workup dramatically increases yield. The crude product is a dark solid with a green luster. Storage of a concentrated hexanes solution at -35° C results in the formation of a lustrous green microcrystalline solid. Yield: 0.86 g (70%). ^{1}H NMR (25 °C, 400 MHz, C_6D_6): δ 3.87 (s, 5H, C_5H_5 Cp-ring), 4.10 (t, 2H, J_{HH} = 1.9 Hz, C-*H* Cp^{dipy} ring), 4.63 (t, 2H, J_{HH} = 1.9 Hz, C-*H Cp^{dipy} ring*) 6.35 (dd, 2H, J_{HH} = 4.2, $^{4}J_{HH}$ = 1.4 Hz, γ-pyrrole C-*H*), 7.32 (br m, 2H, α-pyrrole C-*H*), 7.64 (dd, 2H, J_{HH} = 4.2, $^{4}J_{HH}$ = 1.4 Hz, β-pyrrole C-*H*), 13.94 (s, 1H, pyrrole N-*H*). ^{13}C{^{1}H}NMR (25 °C, 100 MHz, C_6D_6): δ 69.9 (Cp), 71.2 (Cp ring), 74.0 (Cp ring), 83.0 (Cp ring), 116.9 (γ-pyrrole *C*-H), 128.6 (β-pyrrole *C*-H), 141.4, 141.8 (α-pyrrole *C*-H), 143.9.

General procedure for the synthesis of sodium aryldipyrromethenates (**3**)
In a 100 mL round bottom flask, 1 equiv of aryldipyrromethene **2** was dissolved in hexanes (50 mL). In a separate vial, 0.95 equivalents of sodium hexamethyldisilazide (NaHMDS) was dissolved in toluene (9 mL). The NaHDMS solution was added slowly dropwise to the vigorously stirring solution of **2**, resulting in the formation of a fine, insoluble solid. After 1 h, the solid was collected on a medium porosity glass frit, washed with hexanes (20 mL), and dried in vacuo to afford pure, orange powders.

3^{tol}**:** 1.58 g (6.7 mmol) of **2**^{tol} was treated as described with 1.18 g (6.4 mmol) of NaHMDS. The product can be recrystallized from a concentrated DME solution layered with hexanes stored at -35 °C to generate orange crystals. The product crystallizes as the DME solvate **3**^{tol}-0.3DME. Yield: 1.55 g (80%). ^{1}H NMR (25 °C, 400 MHz, C_6D_6/py-d_5): δ 2.17 (s, 3H, tolyl *Me*), 3.07 (s, DME), 3.24 (s, DME), 6.64 (dd, 2H, J_{HH} = 3.7 Hz, $^{4}J_{HH}$ = 0.9 Hz, γ-pyrrole C-*H*), 6.98 (d, 2H, J_{HH} = 8.1 Hz, tolyl C-*H*), 7.01 (dd, 2H, J_{HH} = 3.9 Hz, $^{4}J_{HH}$ = 1.0 Hz, β-pyrrole C-*H*), 7.44 (d, 2H, J_{HH} = 7.9 Hz, tolyl C-*H*), 8.00 (br, 2H, α-pyrrole C-*H*). ^{13}C{^{1}H} NMR (25 °C, 100 MHz, C_6D_6/py-d_5): δ 21.3 (tolyl *Me*), 58.7 (DME), 71.9 (DME), 116.8 (γ-pyrrole *C*-H), 127.5 (tolyl), 131.8 (tolyl), 132.5 (β-pyrrole*C*-H), 137.2, 140.5, 144.4, 150.2, 151.3 (α-pyrrole *C*-H). Anal. Calcd. for $C_{16}H_{13}N_2Na$-0.3DME: C, 72.70; H, 5.76; N, 9.78. Found: C, 72.17; H, 5.85; N, 9.62.
3^{anis}: 0.94 g (3.7 mmol) of **2**^{anis} was treated as described with 0.65 g (3.5 mmol) of NaHMDS. The crude pink-orange product can be recrystallized from a concentrated DME solution layered with

hexanes. Storage of this solution at -35°C yields orange crystals as the solvated product **3**^{anis}-0.75DME. Yield: 0.92 g (77%). ^{1}H NMR (25 °C, 400 MHz, C_6D_6/py-d_5): δ 3.08 (s, 3H, *p*-O*Me*), 3.27 (s, DME), 3.36 (s, DME), 6.63 (dd, 2H, J_{HH} = 3.9, $^{4}J_{HH}$ = 1.0 Hz, γ-pyrrole C-*H*), 6.76 (d, 2H, J_{HH} = 8.6 Hz, anisole C-*H*), 7.02 (dd, J_{HH} = 3.9, $^{4}J_{HH}$ = 1.1 Hz, β-pyrrole C-*H*), 7.45 (d, J_{HH} = 8.7 Hz, , anisole C-*H*), 7.98 (br m, 2H, α-pyrrole C-*H*). ^{13}C{^{1}H} NMR (25 °C, 100 MHz, C_6D_6/py-d_5): δ 54.9 (*p*-O*Me*), 58.7 (DME), 72.0 (DME), 112.4 (anisole), 116.8 (γ-pyrrole *C*-H), 132.2 (β-pyrrole *C*-H), 133.11 (anisole), 135.69, 144.60, 150.80 (α-pyrrole *C*-H), 160.07, one carbon resonance not observed. Anal. Calcd. for $C_{16}H_{13}N_2ONa$-0.75DME: C, 67.14; H, 6.09; N, 8.24. Found: C, 66.96; H, 5.82; N, 8.75.

3^{mes}: 1.0 g (3.8 mmol) of **2**^{mes} was treated as described in the general synthesis with 0.66 g (3.6 mmol) of NaHMDS. The yellow-lime product can be recrystallized from a concentrated Et_2O solution at room temperature. Storage of this solution at -35 °C affords a second crop of crystals. Yield: 0.78 g (76%). ^{1}H NMR (25 °C, 400 MHz, C_6D_6/py-d_5): δ 2.11 (s, 3H, *p-Me*), 2.24 (s, 6H, *o-Me*), 6.55 (dd, 2H, J_{HH} = 3.9, $^{4}J_{HH}$ = 0.9 Hz, γ-pyrrole C-*H*), 6.85 (s, 2H, mesityl C-*H*), 6.89 (dd, 2H, J_{HH} = 3.9, $^{4}J_{HH}$ = 1.1 Hz, β-pyrrole C-*H*), 8.06 (br m, 2H, α-pyrrole C-*H*). ^{13}C{^{1}H} NMR (25 °C, 100 MHz, C_6D_6/py-d_5): δ 20.3 (*o-Me*), 21.2 (*p-Me*), 117.2 (γ-pyrrole *C*-H), 131.0 (β-pyrrole *C*-H), 136.2, 136.9, 139.5, 143.4, 149.0, 151.1 (α-pyrrole *C*-H), two carbon resonances not observed. Anal. Calcd. for $C_{18}H_{17}N_2Na$: C, 76.04; H, 6.03; N, 9.85. Found: C, 74.04; H, 6.30; N, 9.39. Combustion analyses of **3**^{mes} consistently tested low in carbon.

3^{Fc}**:** 0.45 g (1.4 mmol) of 2^{Fc} was treated with 0.24 g (1.3 mmol) of NaHMDS. The brown product can be recrystallized from a concentrated THF solution layered wtih hexanes. Storage of this solution at -35 °C affords dark, brown-red crystals. Yield: 0.41 g (90%). ^{1}H NMR (25 °C, 400 MHz, C_6D_6/py-d_5): δ 3.96 (s, 5H, C_5H_5 Cp-ring), 4.18 (t, 2H J_{HH} = 1.9 Hz, C-*H* Cp^{dipy} ring), 4.94 (t, 2H, J_{HH} = 1.9 Hz, C-*H* Cp^{dipy} ring), 6.71 (dd, 2H, J_{HH} = 3.9, $^{4}J_{HH}$ = 1.0 Hz, γ-pyrrole C-*H*), 7.87 (br m, 2H, α-pyrrole C-*H*), 8.09 (dd, 2H, J_{HH} = 3.8, $^{4}J_{HH}$ = 1.0 Hz, β-pyrrole C-*H*). ^{13}C{^{1}H} NMR (25 °C, 100 MHz, C_6D_6/py-d_5): δ 69.5 (Cp ring), 70.9 (Cp ring), 76.1 (Cp ring), 86.2, 116.4 (γ-pyrrole *C*-H), 130.1 (β-pyrrole *C*-H) , 144.1, 149.0 (α-pyrrole *C*-H), 152.1. Anal. Calcd. for $C_{19}H_{15}FeN_2Na$: C, 65.17; H, 4.32 ; N, 8.00. Found: C, 65.03; H, 4.73, N, 7.66.

General procedure for the synthesis of uranyl bis(aryldipyrromethenates) (4-THF)

In a 20 mL scintillation vial, $UO_2Cl_2(THF)_3$ was dissolved in THF (3 mL). The clear yellow solution was added dropwise to a stirring solution of **3** (2 equiv) in THF (3 mL). The reaction colour turned deep red and was left to stir for 2 h. The product mixture was then filtered through Celite supported on a medium porosity glass frit to give a dark red filtrate. The solvent was removed under vacuum to give **4-THF** as a dichroic, green-red microcrystalline solid. The solid was washed with hexanes (3 × 3 mL) and dried under reduced pressure. Crystals of **4-THF** were obtained by slow diffusion of pentane into a saturated THF:DME (2:1) solution of **4-THF** stored at -30 °C. The instability of these compounds in solution, attributed to the lability of the coordinated THF, precluded full characterization.

4^{tol}-THF: ^{1}H NMR (25 °C, 400 MHz, C_6D_6/THF-d_8): δ 1.43 (THF), 2.12 (s, 6H, Me), 3.68 (THF) 6.43 (br s, 4H), 6.97 (m, 8H, tolyl C-*H*), 7.40 (br s, 4H), 8.05 (br s, 4H).

4^{anis}-THF: ^{1}H NMR (25 °C, 400 MHz, py-d_5): δ 1.75 (THF), 3.80 (*p*-O*Me*, overlapped with THF resonance), 3.83 (THF), 6.22 (s, 4H), 7.15 (d, 4H, anisole C-*H*), 7.34 (s, 4H), 7.78 (d, 4H, anisole C-*H*), 8.12 (s, 4H).

4^{mes}-THF: ^{1}H NMR (25 °C, 400 MHz, py-d_5): δ 1.62 (THF), 2.25 (s, 12H, *o-Me*), 2.36 (s, 6H, *p-Me*), 3.66 (THF), 6.53 (s, 4H), 6.97 (d, 4H), 7.00 (s, 4H, mesityl C-*H*), 7.76 (br s, 4H).

4^{Fc}-THF: ^{1}H NMR (25 °C, 400 MHz, py-d_5): δ 1.42 (THF), 3.56 (THF), 3.96 (s, 10H, C_5H_5 Cp ring), 4.21 (s, 4H, C-*H* Cp^{dipy} ring), 4.88 (s, 4H, C-*H* Cp^{dipy} ring), 6.43 (s, 4H), 7.34 (s, 4H), 7.73 (s, 4H).

General procedure for the synthesis of uranyl bis(aryldipyrromethenates) (4-DMAP)

In a 20 mL scintillation vial, $UO_2Cl_2(THF)_3$ was suspended in Et_2O (3 mL) with 5 equiv of 4-dimethylaminopyridine (DMAP). After 10 min, the yellow suspension transformed into a red-orange mixture. The Et_2O was decanted and the powder resuspended in benzene (6 mL), and this was added to a stirring suspension of **3** (2 equiv) in benzene (10 mL). The reaction colour turned deep red and it was left to stir for 2 h. The product mixture was then filtered through Celite supported on a medium porosity frit to give a dark red filtrate. The Celite filter cake was triturated with benzene to dissolve any remaining product. The solvent was removed under vacuum to give a dichroic, green-red microcrystalline solid. The solid was then washed with cold (-30 °C) Et_2O on a medium porosity glass frit to remove the excess DMAP. X-ray quality single crystals were obtained by slow diffusion of pentane into a saturated THF solution of **4**-DMAP stored at -30 °C.

4^{tol}-DMAP: 0.255 g (0.457 mmol) of $UO_2Cl_2(THF)_3$ was treated as described with 0.279 g (2.28 mmol) of DMAP and 0.400 g (0.917 mmol) of **3**^{tol}. Yield: 0.40 g, (88%). ^{1}H NMR (25 °C, 400 MHz, C_6D_6 /py-d_5): δ 2.13 (s, 6H, tolyl *Me*), 2.21 (s, 6H, DMAP), 6.08 (d, 2H, J_{HH} = 6.4 Hz, DMAP), 6.45 (dd, 4H, J_{HH} = 4.1, γ-pyrrole C-*H*), 6.95 (d, 4H, J_{HH} = 7.8 Hz, tolyl C-*H*), 7.10 (d, 4H, J_{HH} = 4.8 Hz, β-pyrrole C-*H*), 7.48 (d, 4H, J_{HH} = 8.0 Hz, tolyl C-*H*), 7.95 (br s, 4H, α-pyrrole C-*H*), 8.73 (br s, 2H, DMAP). ^{13}C{^{1}H} NMR (25 °C, 100 MHz, C_6D_6/py-d_5): δ 21.2 (tolyl *Me*), 38.3 (DMAP), 107.2 (DMAP), 116.8 (γ-pyrrole *C*-H), 127.7 (tolyl), 131.3 (tolyl]), 132.7, 133.8 (β-pyrrole *C*-H), 137.5, 138.1, 144.5, 151.3, 152.8 (α-pyrrole *C*-H), one carbon resonance not observed. IR (KBr Pellet, cm^{-1}): 531 (w), 578 (w), 283 (w), 620 (w), 647 (w), 653 (w), 713 (w), 730 (m), 770 (m), 797 (m), 848 (w), 873 (w), 883 (m), 897 (w), 920 (m), 937 (w), 963 (m, ν_{asym} U=O), 989 (m), 1007 (m), 1029 (s), 1060 (w), 1069 (w), 1095 (w), 1113 (w), 1166 (m), 1183 (w), 1197 (m), 1227 (m), 1264 (w), 1328 (m), 1373 (s), 1399 (m), 1436 (w), 1537 (s), 1615 (s), 2328 (w), 2365 (w), 2871 (w), 2923 (w), 2965 (w), 3029 (w), 3103 (w). Anal. Calcd. for $C_{32}H_{26}N_4O_2U$-DMAP: C, 54.54; H, 4.23; N, 9.79. Anal. Calcd. for $C_{32}H_{26}N_4O_2U$-1.2DMAP: C, 53.98; H, 4.35; N, 10.15. Found: C, 53.61; H, 4.13; N, 9.51.

4^{anis}-DMAP: 0.282 g (0.506 mmol) of $UO_2Cl_2(THF)_3$ was treated as described with 0.310 g (2.54 mmol) of DMAP and 0.368 g (1 mmol) of **3**^{anis}. Yield: 0.400 g (88%). ^{1}H NMR (25 °C, 400 MHz, C_6D_6/py-d_5): δ 2.20 (s, 6H, DMAP), 3.24 (s, 6H, *p*-O*Me*), 6.09 (d, 2H, J_{HH} = 6.1 Hz, DMAP), 6.49 (d, 4H, J_{HH} = 3.2 Hz, γ-pyrrole C-*H*), 6.75 (d, 4H, J_{HH} = 8.4 Hz, anisole C-*H*), 7.14 (d, 4H, J_{HH} = 3.7 Hz, β-pyrrole C-*H*), 7.50 (d, 4H, J_{HH} = 8.4 Hz, anisole C-*H*), 8.00 (br s, 4H, α-pyrrole C-*H*), 8.79 (br s, 2H, DMAP). ^{13}C{^{1}H} NMR (25 °C, 100 MHz): δ 38.3 (DMAP), 54.9 (*p*-O*Me*), 107.3 (DMAP), 112.9 (anisole), 116.9 (γ-pyrrole *C*-H), 132.8 (anisole), 133.8 (β-pyrrole *C*-H), 144.53, 150.22, 151.12 (DMAP), 152.71 (α-pyrrole *C*-H), 160.36, two carbon resonances not observed. IR (KBr Pellet, cm^{-1}): 421 (w), 463 (w), 470 (w), 532 (w), 583 (w), 616 (w), 645 (w), 667 (w), 716 (w), 734 (w), 757 (w), 774 (w), 808 (m), 837 (w), 874 (w), 882 (w), 897 (w), 916 (m), 935 (w), 963 (w, ν_{asym} U=O), 988 (m), 1007 (s), 1031 (s), 1060 (w), 1095 (m), 1101 (w), 1165 (m), 1169 (m), 1199 (w), 1247 (m), 1291 (w),

1327 (m), 1354 (w), 1374 (s), 1396 (m), 1440 (w), 1458 (w), 1535 (s), 1563 (m), 1605 (s), 1614 (s), 2336 (w), 2355 (w), 2833 (w), 2849 (w), 2863 (w), 2921 (w), 2957 (w), 3028 (w), 3057 (w), 3093 (w), 3421 (w) Anal. Calcd. for $C_{39}H_{36}N_6O_4U$-DMAP: C, 52.58; H, 4.08; N, 9.44. Found: C, 51.99; H, 4.20; N, 8.86.

4^{mes}-DMAP: 0.291 g (0.522 mmol) of $UO_2Cl_2(THF)_3$ was treated as described with 0.319 g (2.6 mmol) of DMAP and 0.293 g (1.04 mmol) of **3**^{mes}. Yield: 0.406 g (85%). ^{1}H NMR (25 °C, 400 MHz, C_6D_6/py-d_5): δ 2.19 (s, 6H, *p-Me*), 2.22 (s, 6H, DMAP), 2.28 (s, 12H, *o-Me*), 6.04 (d, 2H, J_{HH} = 5.7 Hz, DMAP), 6.41 (d, 4H, J_{HH} = 4.9 Hz, γ-pyrrole C-*H*), 6.84 (s, 4H, mesityl C-*H*), 6.98 (d, 4H, J_{HH} = 4.7 Hz, β-pyrrole C-*H*), 7.83 (br s, 4H, α-pyrrole C-*H*), 8.69(br s, 2H, DMAP). ^{13}C{^{1}H} NMR (25 °C, 100 MHz, C_6D_6/py-d_5): δ 20.2 (*o-Me*), 21.2 (*p-Me*), 38.3 (DMAP), 107.2 (DMAP), 117.1 (γ-pyrrole *C*-H), 128.2 (mesityl), 128.6, 131.9 (β-pyrrole *C*-H), 136.8, 137.1, 143.6, 150.4, 152.6 (α-pyrrole *C*-H), two carbon resonances not observed. IR (KBr Pellet, cm^{-1}): 487 (w), 536 (w), 566 (w), 591 (w), 598 (w), 606 (w), 644 (w), 668 (w), 679 (w), 723 (m), 736 (m), 758 (w), 777 (m), 817 (m), 837 (m), 863 (w), 882 (w), 917 (m), 947 (w), 963 (m, ν_{asym} U=O), 987 (m), 1006 (m), 1030 (s), 1063 (w), 1093 (w), 1115 (w), 1165 (m), 1201 (w), 1222 (m), 1234 (m), 1272 (w), 1326 (m), 1337 (w), 1372 (s), 1397 (m), 1439 (w), 1476 (w), 1540 (s), 1567 (w), 1616 (s), 2339 (w), 2357 (w), 2853 (w), 2913 (w), 2943 (w), 3024 (w), 3059 (w), 3084 (w), 3100 (w). Anal. Calcd. for $C_{43}H_{44}N_6O_2U$: C, 56.45; H, 4.85; N, 9.19. Found: C, 56.34; H, 4.92; N, 8.91.

4^{Fc}DMAP: 0.250 g (0.489 mmol) of $UO_2Cl_2(THF)_3$ was treated as described with 0.274 g (2.2 mmol) of DMAP and 0.315 g (0.89 mmol) of **3**^{Fc}. Yield: 0.235 g (50%). ^{1}H NMR (-30 °C, 600 MHz, C_7D_8/py-d_5) δ 2.05 (s, minor isomer), 2.12 (s, minor isomer DMAP), 2.23 (br s, DMAP), 3.84 (s, 5H, minor isomer C_5H_5 Cp ring), 3.98 (s, 5H, minor isomer C_5H_5 Cp ring), 4.00 (s, 10H, major isomer C_5H_5 Cp ring) , 4.11 (s, 2H, minor isomer C-*H* Cp^{dipy} ring), 4.15 (s, 2H, minor isomer C-*H* Cp^{dipy} ring), 4.18 (s, 4H, major isomer C-*H* Cp^{dipy} ring), 4.58 (s, 2H, minor isomer C-*H* Cp^{dipy} ring), 4.78 (s, 2H, minor isomer C-*H* Cp^{dipy} ring), 4.85 (s, 4H, major isomer C-*H* Cp^{dipy} ring), 5.88 (d, 2H, minor isomer J_{HH} = 6.7 Hz, DMAP), 6.03 (br s, DMAP), 6.36, 6.48, 6.66, 7.30 (s, minor isomer), 7.60 (s, minor isomer), 7.79 (s, minor isomer), 7.87 (s, minor isomer), 7.96 (s, major isomer), 8.70 (minor isomer DMAP).^{1}H NMR (30 °C, 600 MHz, C_7D_8/py-d_5): δ 2.12 (s, minor isomer DMAP), 2.28 (br s, DMAP), 3.88 (s, 5H, minor isomer C_5H_5 Cp ring), 3.96 (s, 5H, minor isomer C_5H_5 Cp ring) , 3.97(s, 10H, major isomer C_5H_5 Cp ring), 4.16 (s, 2H, minor isomer C-*H* Cp^{dipy} ring), 4.20 (s, 2H, minor isomer C-*H* Cp^{dipy} ring), 4.23 (s, 4H, major isomer C-*H* Cp^{dipy} ring), 4.61 (s, 2H, minor isomer C-*H* Cp^{dipy} ring), 4.80 (s, 2H, minor isomer C-*H* Cp^{dipy} ring), 4.88 (s, 4H, major isomer C-*H* Cp^{dipy} ring), 6.06(s, DMAP), 6.33, 6.35, 6.48, 6.73, 7.06, 7.31 (s, minor isomer), 7.57 (s, minor isomer), 7.69 (s, minor isomer), 7.79 (s, minor isomer). ^{1}H NMR (80 °C, 600 MHz, C_7D_8/py-d_5): δ 2.12 (s, minor isomer DMAP), 2.36(s, DMAP), 3.95(s, 10H, major isomer C_5H_5 Cp ring), 4.26(s, 4H, major isomer C-*H* Cp^{dipy} ring), 4.89(s, 4H, major isomer C-*H* Cp^{dipy} ring), 6.12(s, DMAP), 6.30 (s, minor isomer) , 6.41 (s, 4H, major isomer (γ-pyrrole *C*-H)), 7.10 (s, 4H, major isomer (β -pyrrole *C*-H)), 7.74(s, minor isomer), 7.75 (s, 4H, major isomer (α -pyrrole *C*-H)). IR (KBr Pellet, cm^{-1}): 413 (w), 425 (w), 481 (m), 499 (m), 529 (w), 571 (w), 597 (m), 610 (m), 655 (m), 656 (m), 664 (w), 677 (m), 730 (m), 769 (m), 806 (m), 831 (m), 883 (m), 914 (m), 950 (w), 963 (m, ν_{asym} U=O), 958 (m), 1004 (s), 1030 (s), 1038 (s), 1047 (m), 1087 (w), 1096 (w), 1105 (w), 1127 (w), 1159 (m), 1200 (m), 1227 (m), 1267 (w), 1311 (m), 1321 (m), 1372 (s), 1392 (s), 1417 (w), 1442 (w), 1459 (w), 1520 (s), 1613 (s) 2331 (w), 2357 (w), 2553 (w), 2852 (w), 2911 (w), 3023 (w), 3083 (w), 3095 (w). Anal. Calcd. for $C_{45}H_{40}Fe_2N_6O_2U$: C, 51.64; H, 3.85; N, 8.03. Found: C, 49.07; H, 4.03; N, 7.88. Combustion analyses of **4**^{Fc}DMAP consistently tested low in carbon.

Acknowledgements

We are grateful to the University of Texas at El Paso, NSF PREM Program (DMR-1205302), and the UT STARS award for support of this work.

Notes and references

1. T. E. Wood and A. Thompson, *Chem. Rev.*, 2007, **107**, 1831-1861.
2. S. A. Baudron, *Dalton Trans.*, 2013, **42**, 7498-7509.
3. A. Loudet and K. Burgess, *Chem. Rev.*, 2007, **107**, 4891-4932.
4. L. Li, J. Han, B. Nguyen and K. Burgess, *J. Org. Chem.*, 2008, **73**, 1963-1970.
5. L. Jiao, C. Yu, T. Uppal, M. Liu, Y. Li, Y. Zhou, E. Hao, X. Hu and M. G. H. Vicente, *Org. Biomol. Chem.*, 2010, **8**, 2517-2519.
6. M. J. Ortiz, I. Garcia-Moreno, A. R. Agarrabeitia, G. Duran-Sampedro, A. Costela, R. Sastre, F. Lopez Arbeloa, J. Banuelos Prieto and I. Lopez Arbeloa, *Phys. Chem. Chem. Phys.*, 2010, **12**, 7804-7811.
7. R. Ziessel, L. Bonardi and G. Ulrich, *Dalton Trans.*, 2006, 2913-2918.
8. V. S. Thoi, J. R. Stork, D. Magde and S. M. Cohen, *Inorg. Chem.*, 2006, **45**, 10688-10697.
9. A. A. Ksenofontov, G. B. Guseva and E. V. Antina, *Mol. Phys.*, 2016, 1-10.
10. L. Yu, K. Muthukumaran, I. V. Sazanovich, C. Kirmaier, E. Hindin, J. R. Diers, P. D. Boyle, D. F. Bocian, D. Holten and J. S. Lindsey, *Inorg. Chem.*, 2003, **42**, 6629-6647.
11. E. T. Hennessy and T. A. Betley, *Science*, 2013, **340**, 591.
12. S. R. Halper and S. M. Cohen, *Inorg. Chem.*, 2005, **44**, 486-488.
13. J. R. Stork, V. S. Thoi and S. M. Cohen, *Inorg. Chem.*, 2007, **46**, 11213-11223.
14. C. P. Baird and T. J. Kemp, *Prog. React. Kinet.*, 1997, **22**, 87-139.
15. J.-C. G. Bunzli and C. Piguet, *Chem. Soc. Rev.*, 2005, **34**, 1048-1077.
16. Y. Hasegawa and T. Nakanishi, *RSC Adv.*, 2015, **5**, 338-353.
17. H. S. He, *Coord. Chem. Rev.*, 2014, **273**, 87-99.
18. B. S. Harrison, T. J. Foley, A. S. Knefely, J. K. Mwaura, G. B. Cunningham, T. S. Kang, M. Bouguettaya, J. M. Boncella, J. R. Reynolds and K. S. Schanze, *Chem. Mater.*, 2004, **16**, 2938-2947.
19. R. F. Ziessel, G. Ulrich, L. Charbonnière, D. Imbert, R. Scopelliti and J.-C. G. Bünzli, *Chem. Eur. J.*, 2006, **12**, 5060-5067.
20. J. R. Pankhurst, N. L. Bell, M. Zegke, L. N. Platts, C. A. Lamfsus, L. Maron, L. S. Natrajan, S. Sproules, P. L. Arnold and J. B. Love, *Chem. Sci.*, 2016, DOI: 10.1039/C6SC02912D.
21. B. J. Littler, M. A. Miller, C.-H. Hung, R. W. Wagner, D. F. O'Shea, P. D. Boyle and J. S. Lindsey, *J. Org. Chem.*, 1999, **64**, 1391-1396.
22. C.-H. Lee and J. S. Lindsey, *Tetrahedron*, 1994, **50**, 11427-11440.

23. T. Rohand, E. Dolusic, T. H. Ngo, W. Maes and W. Dehaen, *ARKIVOC*, 2007, **2007**, 307-324.
24. C. Brückner, V. Karunaratne, S. J. Rettig and D. Dolphin, *Can. J. Chem.*, 1996, **74**, 2182-2193.
25. C. Trinh, K. Kirlikovali, S. Das, M. E. Ener, H. B. Gray, P. Djurovich, S. E. Bradforth and M. E. Thompson, *J. Phys. Chem. C*, 2014, **118**, 21834-21845.
26. C. Bruckner, Y. J. Zhang, S. J. Rettig and D. Dolphin, *Inorg. Chim. Acta*, 1997, **263**, 279-286.
27. A. A.-S. Ali, J. Cipot-Wechsler, S. M. Crawford, O. Selim, R. L. Stoddard, T. S. Cameron and A. Thompson, *Can. J. Chem.*, 2010, **88**, 725-735.
28. A. B. Scharf and T. A. Betley, *Inorg. Chem.*, 2011, **50**, 6837-6845.
29. A. K. Burrell, G. Hemmi, V. Lynch and J. L. Sessler, *J. Am. Chem. Soc.*, 1991, **113**, 4690-4692.
30. J. L. Sessler, D. Seidel, A. E. Vivian, V. Lynch, B. L. Scott and D. W. Keogh, *Angew. Chem. Int. Ed.*, 2001, **40**, 591-594.
31. T. Furuyama, Y. Ogura, K. Yoza and N. Kobayashi, *Angew. Chem. Int. Ed.*, 2012, **51**, 11110-11114.
32. J. L. Sessler and A. Gebauer, *Chem. Commun.*, 1998, 1835-1836.
33. P. L. Arnold, A. J. Blake, C. Wilson and J. B. Love, *Inorg. Chem.*, 2004, **43**, 8206-8208.
34. P. J. Melfi, S. K. Kim, J. T. Lee, F. Bolze, D. Seidel, V. M. Lynch, J. M. Veauthier, A. J. Gaunt, M. P. Neu, Z. Ou, K. M. Kadish, S. Fukuzumi, K. Ohkubo and J. L. Sessler, *Inorg. Chem.*, 2007, **46**, 5143-5145.
35. V. W. Day, T. J. Marks and W. A. Wachter, *J. Am. Chem. Soc.*, 1975, **97**, 4519-4527.
36. S. Fortier and T. W. Hayton, *Coord. Chem. Rev.*, 2010, **254**, 197-214.
37. M. J. Sarsfield, M. Helliwell and J. Raftery, *Inorg. Chem.*, 2004, **43**, 3170-3179.
38. J.-C. Berthet, M. Nierlich and M. Ephritikhine, *Dalton Trans.*, 2004, 2814-2821.
39. J.-C. Berthet, M. Nierlich and M. Ephritikhine, *Chem. Commun.*, 2003, 1660-1661.
40. R. Copping, B. Jeon, C. D. Pemmaraju, S. Wang, S. J. Teat, M. Janousch, T. Tyliszczak, A. Canning, N. Grønbech-Jensen, D. Prendergast and D. K. Shuh, *Inorg. Chem.*, 2014, **53**, 2506-2515.
41. J. M. Ribo, J.-A. Farrera, J. Claret and K. Grubmayr, *Bioelectroch. Bioener.*, 1992, **29**, 1-17.
42. E. R. King and T. A. Betley, *Inorg. Chem.*, 2009, **48**, 2361-2363.
43. N. A. Smith, G. S. Cerefice and K. R. Czerwinski, *J. Radioanal. Nucl. Chem.*, 2013, **295**, 1553-1560.
44. I. V. Sazanovich, C. Kirmaier, E. Hindin, L. Yu, D. F. Bocian, J. S. Lindsey and D. Holten, *J. Am. Chem. Soc.*, 2004, **126**, 2664-2665.
45. J. Jia, Y. Cui, Y. Li, W. Sheng, L. Han and J. Gao, *Dyes Pigm.*, 2013, **98**, 273-279.
46. M. P. Wilkerson, C. J. Burns, R. T. Paine and B. L. Scott, *Inorg. Chem.*, 1999, **38**, 4156-4158.
47. SMART, Version 2.1 ed.; Bruker AXS Inc.: Madison, WI, 2005.
48. SAINT, Version 7.34a ed.; Bruker AXS Inc.: Madison, WI, 2005.
49. R. Blessing, *Acta Cryst. A*, 1995, **51**, 33-38.
50. G. M. Sheldrick, 6.12 ed.; Bruker Analytical X-Ray Systems, Inc.: Madison, WI, 2001.
51. O. V. Dolomanov, L. J. Bourhis, R. J. Gildea, J. A. K. Howard and H. Puschmann, *J. Appl. Cryst.*, 2009, **42**, 339-341.
52. J. F. Gallagher and E. Moriarty, *Acta Cryst. C*, 1999, **55**, 1079-1082.

View Article Online
DOI: 10.1039/C7DT00150A

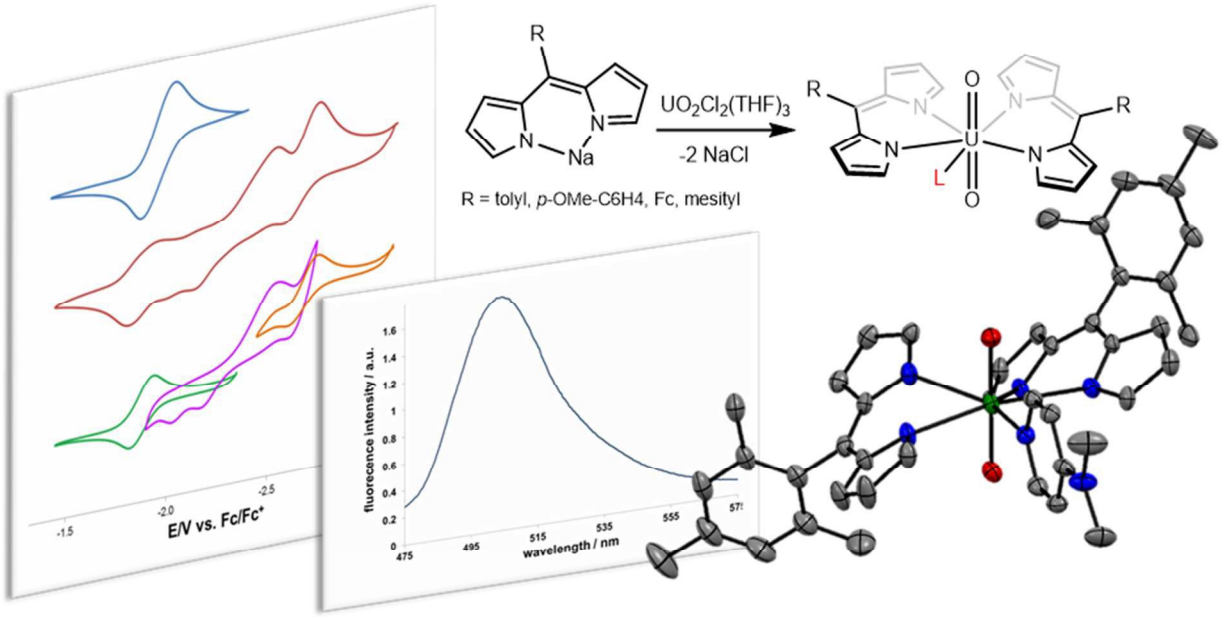

Using an improved, chromatography-free dipyrrin synthesis, a new family of actinide dipyrrinate complexes has been synthesized.